Letters in Drug Design & Discovery, 2016, *13*, 441-450

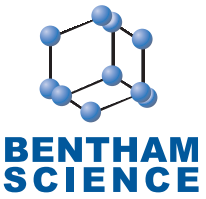

BENTHAM SCIENCE

Endothelium Dependent and Independent Mechanisms of Vasorelaxant Activity of Synthesized 2,5-disubstituted-1,3,4-oxadiazole Derivatives in Rat Thoracic Aorta – *Ex vivo* and Molecular Docking Studies

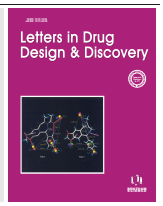

Zenab Attari[1], Jayesh Mudgal[1], Pawan G Nayak[1], Nandakumar Krishnadas[1], Revathi Rajappan[2] and N. Gopalan Kutty[1,*]

[1]*Department of Pharmacology, Manipal College of Pharmaceutical Sciences, Manipal University, Manipal, Karnataka, India*

[2]*Department of Pharmaceutical Chemistry, Manipal College of Pharmaceutical Sciences, Manipal University, Manipal, Karnataka, India*

N. Gopalan Kutty

Abstract: ***Background*:** Vasoconstriction is a major pathological feature of cardiovascular diseases involving endothelium dependent and independent mechanisms. Oxadiazole moiety appeared to be effective in various pathologies.

***Objective*:** The aim of the study was to synthesize and evaluate the mechanism of vasorelaxation exhibited by synthesized oxadiazole derivatives.

***Method*:** The 2,5-disubstituted-1,3,4-oxadiazole derivatives were synthesized by an efficient and simple method. The derivatives were investigated for their *ex-vivo* vasorelaxant action on intact/denuded endothelium rat aortic rings precontracted with norepinephrine/ phenylephrine/KCl.

***Results*:** The contractions induced in the aortic rings by the addition of cumulative concentrations of norepinephrine, phenylephrine, KCl and calcium were significantly antagonized by a derivative, OXD-Z2. In another experiment, verapamil pretreatment inhibited phenylephrine and Ca^{2+}-induced aortic contractions and OXD-Z2 did not alter verapamil-induced inhibition. This indicated the role of L-type Ca^{2+}-channels in the OXD-Z2-induced vasorelaxation via inhibition of calcium influx. Further, atropine (muscarinic receptor antagonist), L-NAME (NO synthase inhibitor) and methylene blue (non-selective cGMP inhibitor) inhibited OXD-Z2-induced relaxation in other sets of experiments. These results indicate that OXD-Z2 also mediates vasorelaxation through NO release by muscarinic receptor activation. In addition, the molecular docking studies showed that OXD-Z2 interacts with L-type Ca^{2+}-channel, muscarinic (M_2) receptor and eNOS.

***Conclusion*:** Thus, it is deduced from the above findings that the vasorelaxant activity of OXD-Z2 involves muscarinic receptor-mediated nitric oxide release in addition to direct inhibition of L-type Ca^{2+}-channels.

Keywords: 2,5-disubstituted-1,3,4-oxadiazoles, aortic rings, endothelium, vasorelaxation, hypertension.

1. INTRODUCTION

Endothelial dysfunction is the important underlying pathological feature of cardiovascular diseases viz. hypertension, coronary artery disease, chronic heart failure, peripheral artery disease, diabetes, and chronic renal failure. Injury to endothelia of blood vessels results in imbalance in cardiovascular homeostasis, eventually leading to endothelial dysfunction. This is characterized by pro-inflammatory states, pro-thrombotic properties and reduced vasodilatation [1, 2].

Oxadiazole scaffold is a versatile pharmacophore, which possesses diverse activities such as hypoglycaemic, vasorelaxant and antihypertensive [3, 4]. A previous study in our laboratory demonstrated the vasorelaxant activity of 2, 5-disubstituted-1, 3, 4-oxadiazole due to its ability to inhibit calcium flux [5]. The present work was aimed to explore if oxadiazole derivatives exert their vasorelaxant action through mechanisms beyond calcium channel inhibition. Thus, eight 2,5-disubstituted-1,3,4-oxadiazole derivatives were synthesized by a simple method and evaluated for their vasorelaxant actions in the rat thoracic aorta followed by assessment of the involvement of endothelium-dependent or –indepen-dent mechanism in their vasorelaxant action.

2. EXPERIMENTAL

2.1. Synthesis

The oxadiazole derivatives (coded as OXD-Z1 to OXD-Z8) were synthesized by a well-established two-step method with some modifications [5]. Briefly, isoniazid (b)

*Address correspondence to this author at the Department of Pharmacology, Manipal College of Pharmaceutical Sciences, Manipal University, Manipal - 576104, Karnataka, India; Tel: +91-820-2922482; Extn: 322; Fax: +91-820-2571998; E-mail: ng.kutty@manipal.edu

1875-628X/16 $58.00+.00

Table 1. Characterization of 2,5-disubstituted-1,3,4-oxadiazole derivatives.

Benzaldehyde Derivatives	Compound Code	Molecular Formula	R1	R2	M_w	MP(ºC)
p-Anisaldehyde	OXD-Z1	$C_{16}H_{15}O_3N_3$	H	OCH_3	297	98
p-Tolualdehyde	OXD-Z2	$C_{16}H_{15}O_2N_3$	H	CH_3	281	102
p-Fluoro-benzaldehyde	OXD-Z3	$C_{15}H_{12}FO_2N_3$	H	F	285	104
p-Chloro-benzaldehyde	OXD-Z4	$C_{15}H_{12}ClO_2N_3$	H	Cl	301	114
p-Hydroxy-benzaldehyde	OXD-Z5	$C_{17}H_{15}O_4N_3$	H	$OCOCH_3$	325	210
p-Dimethylamino-benzaldehyde	OXD-Z6	$C_{17}H_{18}O_2N_4$	H	$(CH_3)_2N$	310	49
Vanillin	OXD-Z7	$C_{18}H_{17}O_5N_3$	OCH_3(*m*-)	$OCOCH_3$	355	174
Salicylaldehyde	OXD-Z8	$C_{17}H_{15}O_4N_3$	$OCOCH_3$	H	325	152

was dissolved in methanol and *ortho*- or *para*- substituted benzaldehyde (a) was added to the methanolic solution along with a few drops of glacial acetic acid (Table **1**). The mixture was refluxed for 30 minutes. The intermediate product, Schiff base (c) was filtered and recrystallized from alcohol. Schiff base was heated for 5h with acetic anhydride on a water bath.The reaction mixture (d) was then poured on to crushed ice in a beaker. The solid that separated was recrystallized from boiling water. The schematic representation of synthesis is given in Fig. (**1**).

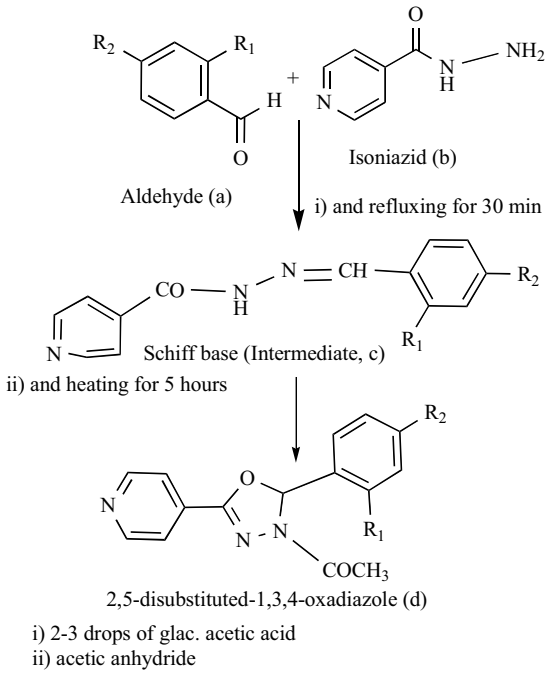

1a. Schematic representation of synthesis of 2,5-disubstituted-1,3,4-oxadiazole derivatives

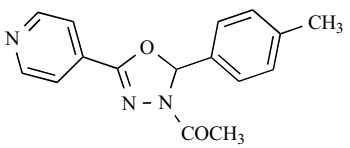

Fig. (1). 1b. Structure of 2,5-disubstituted-1,3,4-oxadiazole derivative, OXD-Z2.

The characteristic properties of oxadiazole derivatives were established through chemical, chromatographic and spectroscopic methods. The strucures of the 1,3.4-oxadiazole derivatives (OX-Z1 and OX-Z2) were confirmed through IR, NMR and mass spectrometry. The remaining compounds were characterized through their IR spectral data.

1. OXD-Z1 (1-[2-(4-methoxyphenyl)-5-(pyridine-4-yl)-1,3,4-oxadiazol-3(2H)-yl] ethanone)

Mass - 297$[M]^+$, 298$[M+1]^+$, 255 m/z, 133 m/z.

^{1}H NMR - 8.6 [d, 2H, -N(C<u>H</u>)$_2$-)]; 6.8, 7.3, 7.6 [d, 6H, Ar-<u>H</u>]; 6.9 [s, 1H, O-C(<u>H</u>)-N($COCH_3$)N]; 3.75 [s, 3H, -O$C\underline{H}_3$]; 2.32 [s, 3H, -$COC\underline{H}_3$].

IR (KBr, cm^{-1}) - 3047.63 (-Ar), 2933.83-2833.52 (-CH- of Ar), 1670.41 (-$COCH_3$), 1618.83-1410.10 (-C=N of Pyridine), 1259.56 (C-O-C asymmetric), 1170.83 (-OCH_3), 1068.60 (C-O-C symmetric).

2. OXD-Z2 (*1-[2-(4-methylphenyl)-5-(pyridine-4-yl)-1,3,4-oxadiazol-3(2H)-yl] ethanone*)

Mass - 281 $[M]^+$, 239 m/z, 78 m/z

^{1}H NMR - 8.8 [d, 2H, -N(C<u>H</u>$_2$)-]; 7.2, 7.3, 7.7 [d, 6H, Ar-<u>H</u>]; 7.07 [s, 1H, O-C(<u>H</u>)N($COCH_3$)N]; 2.36 [s, 3H, Ar-$C\underline{H}_3$]; 2.33 [s, 3H, -$COC\underline{H}_3$]

IR (KBr, cm^{-1}) - 3032.20 (-Ar), 2920.32 (-CH- of Ar), 2845.10 (-CH_3), 1670.41 (-$COCH_3$), 1600.97-1410.01 (-C=N of pyridine), 1257.63 (C-O-C asymmetric), 1066.67 (C-O-C symmetric)

3. OXD-Z3 (*1-[2-(4-fluorophenyl)-5-(pyridine-4-yl)-1,3,4-oxadiazol-3(2H)-yl] ethanone*)

IR (KBr, cm^{-1}) - 3182.65 (-Ar), 2916.47 (-CH- of Ar), 16565.91 (-$COCH_3$), 1406.15 (-C=N of Pyridine), 1298.14 (C-O-C asymmetric), 1149.61 (-F), 1064.74 (C-O-C symmetric).

4. OXD-Z4 (*1-[2-(4-chlorophenyl)-5-(pyridine-4-yl)-1,3,4-oxadiazol-3(2H)-yl] ethanone*)

IR (KBr, cm^{-1}) - 3032.20 (-Ar), 2850.88 (-CH- of Ar), 1668.48 (-$COCH_3$), 1408.08 (-C=N of Pyridine), 1261.59 (C-O-C asymmetric), 1082.10 (C-O-C symmetric), 825.56 (-Cl).

5. OXD-Z5 (*4-[3-acetyl-5-(pyridine-4-yl)-2,3-dihydro-1,3,4-oxadiazol-2-yl] phenyl acetate*)

IR (KBr, cm^{-1}) - 3037.99 (-Ar), 1743.71 (-$OCOCH_3$), 1662.69 (-$COCH_3$), 1419.66 (-C=N of Pyridine), 1222.91 (C-O-C asymmetric), 1058.96 (C-O-C symmetric).

6. OXD-Z6 (*1-[2-(4-dimethylaminophenyl)-5-(pyridine-4-yl)-1,3,4-oxadiazol-3(2H)-yl] ethanone*)

IR (KBr, cm^{-1}) - 2906.82 (-Ar), 2820.02 (-CH- of Ar), 1660.77 (-$COCH_3$), 1437.02 (-C=N of Pyridine), 1232.55 (C-O-C asymmetric), 1163.11 (tertiary amine), 1064.74 (C-O-C symmetric).

7. OXD-Z7 (4-*[3-acetyl-5-(pyridine-4-yl)-2,3-dihydro-1,3,4-oxadiazol-2-yl]-2-methoxyphenyl acetate*)

IR (KBr, cm^{-1}) - 3072.71 (-Ar), 2956.97 (-CH- of Ar), 1764.93 (-$OCOCH_3$), 1656.91 (-$COCH_3$), 1415.80 (-C=N of Pyridine), 1213.27 (C-O-C asymmetric), 1161.19 (-OCH_3), 1064.74 (C-O-C symmetric).

8. OXD-Z8 (*2-[3-acetyl-5-(pyridine-4-yl)-2,3-dihydro-1,3,4-oxadiazol-2-yl] phenyl acetate*)

IR (KBr, cm^{-1}) - 3037.99 (-Ar), 2976.26 (-CH- of Ar), 1759.14 (-$OCOCH_3$), 1664.62 (-$COCH_3$), 1415.80 (-C=N of Pyridine), 1265.35 (C-O-C asymmetric), 1064.74 (C-O-C symmetric).

2.2. Drugs and Chemicals

As oxadiazole derivatives are water-insoluble at room temperature, they were dissolved in dimethyl sulfoxide (DMSO) and subsequent dilutions were made from stock solution. The drugs and chemicals used in the study were purchased from standard chemical suppliers.

2.3. Animals

Male Wistar rats, weighing 200-250 g were employed for the study. The rats were housed 3 per cage and maintained in the Central Animal Research Facility (CARF), Manipal University. The temperature of the room was maintained at 23±2°C with a 12 h light-dark cycle. The animal experiments were carried out according to the guidelines of CPCSEA, with the approval of the Institutional Animal Ethical Committee (IAEC) (vide letter # IAEC/KMC/54/2009-2010).

2.3.1. Preparation of Aortic Rings for Tension Measurement

The experiment was carried out by the method as previously established in our laboratory setup [5]. Rats were sacrificed and the descending thoracic aorta was dissected after removing the surrounding connective tissue and fat. The bathing fluid for aorta was the Kreb's solution of the composition: 118mM NaCl, 4.7mM KCl, 1.2mM $MgSO_4$, 1.2mM KH_2PO_4, 2.4mM $CaCl_2$, 25mM $NaHCO_3$ and 11mM glucose. The aortic rings (2.5 mm) were mounted in an organ bath filled with 20 ml Kreb's solution at a resting tension of 2.0 g. The bath was maintained at 37ºC and aerated with a mixture of 95% O_2 and 5% CO_2 gas. Isometric contractions and relaxations were recorded using a force displacement transducer (model MLT050/A, AD Instruments, Australia) and result was analyzed using AD Instruments Power Lab software. The aortic rings were equilibrated for 120 minutes in Kreb's solution, which was changed once every 20 minutes. The aortic rings were denuded by removing endothelium using a 25-gauge needle tip. The absence of Ach-induced relaxation was considered an indication of denudation.

2.3.2. Vasorelaxant Effect of OXD-Z2 on Norepinephrine (NE), Phenylephrine (PE) and KCl-induced Precontraction in Rat Aortic Rings with and Without Endothelium

The contractions were induced by PE (1μM), NE (300nM) and KCl (60mM) in the aortic rings with or without endothelium. The effect of OXD-Z2 was recorded on pre-contracted aorta after cumulative addition of OXD-Z2 (10nM to 3mM) directly to the organ bath.

2.3.3. Effect of OXD-Z2 on Cumulative Concentration-Response Curve of PE, NE and KCl

Cumulative concentration-response curves (CRCs) for PE (10pM to 300nM), NE (10pM to 300nM) and KCl (10mM to 80mM) were obtained without and with incubating denuded aortic rings with OXD-Z2 (100nM and 300nM) for 20 minutes. The effect of OXD-Z2 on the cumulative CRCs of PE, NE and KCl was determined by comparing % contraction in the presence and absence of OXD-Z2.

2.3.4. Effect of OXD-Z2 on Cumulative Concentration-Response of Ca^{2+}-induced Contraction in Calcium Free Depolarized Kreb's Solution

The denuded aortic rings were incubated in calcium-free Kreb's solution for ten minutes, followed by replacement of the solution with Ca^{2+}-free isotonic depolarizing solution containing a high concentration of K^+ (100mM KCl). The tissues were then incubated with OXD-Z2 (100nM and 300nM) for 15 minutes followed by recording of CRCs of Ca^{2+} (1μM to 30mM). The effect of OXD-Z2 on the cumulative CRCs of Ca^{2+} was determined by comparing % contraction in the presence and absence of OXD-Z2.

2.3.5. Effect of OXD-Z2 on Cumulative Concentration-Response of PE and Ca^{2+} in the Aortic Rings Pretreated with Verapamil

The CRC was recorded to assess the possible role of L-type calcium channels (Ca^{2+}-channels) in the OXD-Z2-induced attenuation of contraction by PE and Ca^{2+}. The aortic rings were incubated with verapamil (10μM) or OXD-Z2 (1μM) with verapamil (10μM) for 20 minutes before cumulative CRCs of PE and Ca^{2+}. The effect of OXD-Z2 on the cumulative CRCs of PE and Ca^{2+}in the presence of verapamil was determined by comparing % contraction in the presence and absence of OXD-Z2.

2.3.6. Investigation of Mechanisms Involving Endothelium

The CRCs were obtained after addition of different inhibitors to assess the involvement of mechanisms other than Ca^{2+} in OXD-Z2-induced vasorelaxation. The aortic rings were incubated with different inhibitors L-NAME (N^G-nitro-

L-arginine-methyl ester) (10μM, a non-selective NOS inhibitor), indomethacin (10μM, a COX inhibitor), glibenclamide (10μM, an ATP-sensitive K^+-channel blocker), atropine (10μM, muscarinic receptor antagonist) or methylene blue (10μM, a guanylate cyclase inhibitor) and then the cumulative concentrations of OXD-Z2 (10nM to 3mM) were added to record relaxation of the precontracted aortic rings.

2.4. Data Analysis

All vasorelaxation responses recorded, were expressed as percentage relaxation from the pre-constricted response of PE, NE, KCl or calcium. Data are expressed as mean ± SEM of 3 experiments. Contractile responses to NE, PE, KCl and Ca^{2+} were expressed as the percentages of the maximum contraction. E_{max} is the maximum % contraction induced by PE, NE, KCl or Ca^{2+}. The pD_2 and EC_{50} values were calculated by non-linear regression analysis using Prism demo version 6.0; Graph Pad Software, San Diego, CA, USA. The results were analyzed by the "Student's t-test" and ANOVA followed by post hoc "Tukey's test" at the significance level $p< 0.05$, where applicable.

The pD_2 values were calculated by the formula,

$$pD_2 = pD_x + Log[(E_{Am}/E_{Bm})-1]$$

where, pD_x is negative log[OXD-Z2]M, E_{Am} is % maximum contraction induced by contractile agent/agonist, E_{Bm} is % maximum contraction induced by contractile agent/agonist in presence of OXD-Z2. pD_2 value indicates a non-competitive antagonism.

2.5. Molecular Docking

Molecular docking studies were carried out by using V.Life MDS 4.2 software. The PLP function was incorporated by the MDS V.Life Science software in the GRIP docking method, which calculates the ligand-receptor binding affinity in terms of the PLP score. The PLP score was designed to enable flexible docking of ligand to perform a full conformational and positional search within a rigid binding site. All the optimized conformers were docked into active binding site of L-type Ca^{2+}-channel (PDB ID 1T0J) [6] and eNOS (PDB ID 3HR4 and 3NOS) [7] and for muscarinic receptor, the derivative was docked to M_2 receptor (PDB ID 3UON). M_2 receptor (PDB ID 3UON) was used as a template for docking studies as the crystal structure of M_1 receptor was not available [8]. Water molecules and HET ATOM-like bound ligand data were removed from the PDB file of proteins during docking study. The crystal structure was refined using V.Life Science's MDS 4.2 software. The refinement of the crude PDB structure of receptor was done by completing the incomplete residues. The co-crystallized ligand lying within the receptor was modified by assigning missing bond order and hybridization states. The side chain hydrogens were then added to the crystal structure and their positions were optimized up to the rms gradient 1 by aggregating the other part of the receptor. The optimized receptor was then saved as mol file and used for docking simulation. The 2D structure of the compound OXD-Z2 was built and then converted into the 3D with the help of VLife MDS 4.2 software. The 3D structures were then energetically minimized up to the rms gradient of 0.01 using Merck Molecular Force Field (MMFF). Conformers of compounds were then generated by Monte Carlo method. In doing so, all rotatable bonds of the ligand were selected and number of seeds used for searching the conformational space was set 5. All the conformers were then energetically minimized up to the rms gradient of 0.01 and then saved in separate folder. The active site selection was done by choosing the cavity having maximum hydrophobic surface area. The docking simulation was done using GRIP docking. The parameters fixed for docking simulation was like this-number of placement: 50, rotation angle of: 10°, exhaustive method, scoring function: dock score. After docking simulation, the best docked conformer of the ligand and receptor were merged and their complex was then energetically optimized by defining radius of 10 Å measured from the docked ligand. Stepwise energy optimization was done by first hydrogens; second side chains and finally the backbone of receptor. The optimized complexes were then checked for various interaction of ligand with receptor like hydrogen bonding, hydrophobic bonding and Van der Waals' interaction etc. The binding affinity was evaluated by the binding free energy (ΔGb, kcal/mol) and binding interactions [10].

3. RESULTS

3.1. Synthesis

The list of eight oxadiazole derivatives synthesized and their chemical identities are depicted in Table **1**.

3.2. Vasorelaxant Effect of OXD-Z2 on Phenylephrine (PE), Norepinephrine (NE) and KCl-induced Precontraction in Rat Aortic Rings with and Without Endothelium

NE (300nM), PE (1μM) and KCl (60mM) produced a sub-maximal contraction of aortic ring. All the oxadiazole derivatives were analyzed for vasorelaxant activity in PE-contracted aortic ring. OXD-Z1 and OXD-Z3 to OXD-Z8 failed to produce satisfactory vasorelaxation in thoracic aortic rings (data not shown). However, cumulative addition of OXD-Z2 (10nM to 3mM) produced a significant vasorelaxation in the pre-contracted aortic rings (Fig. **2**). pEC_{50} and EC_{50} values of OXD-Z2 are depicted in Table **2**.

3.3. Effect of OXD-Z2 on Cumulative Concentration-Response Curve of PE, NE and KCl

The concentration-dependent contraction of aortic ring was obtained by the cumulative addition of PE (10pM to 300nM), NE (10pM to 300nM) and KCl (10mM to 80mM). Incubation of the aortic ring with OXD-Z2 (100nM and 300nM) shifted the CRCs of PE, NE and KCl towards right with change in E_{max} values, indicating antagonistic or vasodilatory activity of OXD-Z2 (Fig. **3**). The shift in CRCs of PE and KCl in the presence of OXD-Z2 (100nM) and OXD-Z2 (300nM) was significantly different in its absence ($p<0.05$) (EC_{50} ratio are given in Table **3**). The shift of CRC of NE was significant in the presence of 300nM but not 100nM of OXD-Z2. However, no difference was observed between mean values of OXD-Z2 at the concentrations, 100 and 300nM

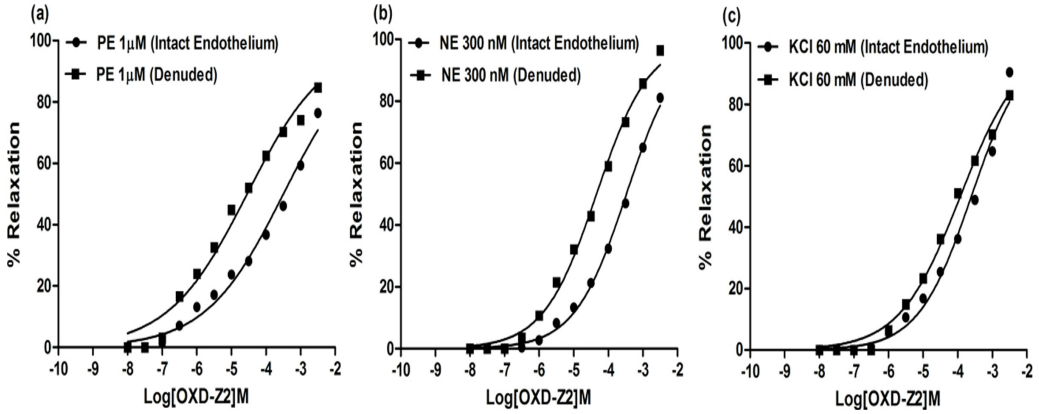

Values are expressed as Mean ± SEM

Fig. (2). Vasorelaxant effect of OXD-Z2 in endothelium intact and denuded aortic rings pre-contracted with **(a)** PE (1μM), **(b)** NE (300nM) and **(c)** KCl (60mM).

Table 2. $EC_{50}$and pEC_{50} values showing vasorelaxant effect of OXD-Z2 on aortic rings pre-contracted with PE, NE and KCl.

	pEC_{50} [a]		EC_{50} (10^{-4} M) [b]	
OXD-Z2 Against	**With Endothelium**	**Without Endothelium**	**With Endothelium**	**Without Endothelium**
PE	3.49 ± 0.06 R^2=0.98	4.54 ± 0.08 R^2=0.98	3.2 (2.2-4.5)	0.28 (0.18-0.43)
NE	3.47 ± 0.02 R^2=0.99	4.33 ± 0.04 R^2=0.99	3.3 (2.9-3.7)	0.45 (0.37-0.56)
KCl	3.61 ± 0.06 R^2=0.98	3.93 ± 0.04 R^2=0.99	2.4 (1.7-3.3)	1.1 (0.9-1.4)

[a] pEC_{50} values are mean ± SEM of 3 experiments
[b] EC_{50} values are expressed in 10^{-4} M concentration and 95% confidence interval in parentheses

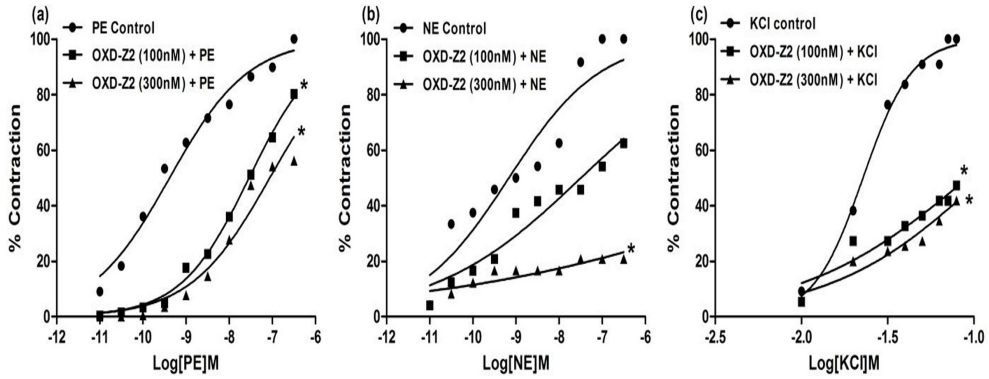

*p<0.05 showed significant difference as compared to control group

Fig. (3). Effect of OXD-Z2 (100 & 300nM) on concentration-response curves of **(a)** PE, **(b)** NE and **(c)** KCl in rat aortic rings.

Table 3. EC_{50} ratio and E_{max} of cumulative concentration-response curve of PE, NE, KCl and Ca^{2+} in presence of OXD-Z2.

	EC_{50} Ratio [a]		E_{max}% [b]	
CRC	**OXD-Z2 (100nM) Against**	**OXD-Z2 (300nM) Against**	**OXD-Z2 (100nM) Against**	**OXD-Z2 (300nM) Against**
PE	72.21	200.1	80.25	50.66
NE	41.46	6426	62.5	20.83
KCl	3.6	4.2	47.27	41.82
Ca^{2+}	43.77	108.6	61.19	51.40

[a] EC_{50} ratio is the ratio of EC_{50} in presence of OXD-Z2 divided by EC_{50} of contractile agonist
[b] E_{max} is the maximum contraction by contractile agonist in presence of OXD-Z2

in PE, NE or KCl precontracted rings. The pD2 values of OXD-Z2 (100nM) and OXD-Z2 (300nM) against PE-induced contraction were found to be 7.24 and 7.27, respectively. The pD2 values of OXD-Z2 (100nM) and OXD-Z2 (300nM) against NE-induced contractions were found to be 7.6 and 10.3, respectively. The pD2 values of OXD-Z2 (100nM) and OXD-Z2 (300nM) against KCl-induced contractions were found to be 8.12 and 7.89, respectively.

3.4. Effect of OXD-Z2 on Cumulative Concentration-Response Curve of Ca^{2+}-induced Contraction in Ca^{2+}-free Depolarized Kreb's Solution

Cumulative addition of Ca^{2+} (1μM to 30mM) produced a concentration-dependent contraction of the aortic ring suspended in the Ca^{2+}-free depolarizing Kreb's solution containing 100mM KCl. Incubation of the aortic ring with OXD-Z2 (100nM and 300nM) significantly antagonized (Fig. **4**) the Ca^{2+}-induced contraction at $p<0.05$. The pD2 values of OXD-Z2 (100nM) and OXD-Z2 (300nM) against Ca^{2+}-induced contraction were found to be 7.63 and 7.44, respectively. EC_{50} ratio indicated shift in the CRC of Ca^{2+} in the presence of OXD-Z2 from CRC of Ca^{2+} without OXD-Z2 with change in E_{max} value (Table **3**).

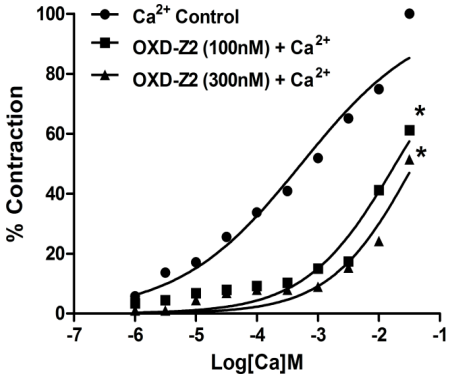

*p<0.05 showed significant difference as compared to control group

Fig. (4). Effect of OXD-Z2 (100nM & 300nM) on concentration response curves of Ca^{2+} in rat aortic rings.

3.5. Effect of OXD-Z2 on Cumulative Concentration-Response Curves of PE and Ca^{2+} in the Aortic Rings Pretreated with Verapamil

Cumulative addition of PE (10pM to 3μM) and Ca^{2+} (1μM to 30mM) resulted in a concentration-dependent contraction of endothelium-denuded aortic ring. PE and Ca^{2+}-induced (Fig. **5**) contractions in aortic ring were inhibited by pretreatment with verapamil (10μM) as well as OXD-Z2 (1μM) with verapamil (10μM). No statistical significant difference was observed between the two groups, verapamil and OXD-Z2 with verapamil.

3.6. Effect of OXD-Z2 on Vascular Tonus in Presence of Inhibitors

Incubation of endothelium-intact aortic rings with inhibitors, atropine, methylene blue and L-NAME was found to significantly inhibit OXD-Z2-induced relaxation, whereas, indomethacin and glibenclamide did not affect the OXD-Z2-induced relaxation (Fig. **6**). The shift in EC_{50} ratio indicates the attenuation of OXD-Z2-induced vasorelaxation in presence of inhibitors. The EC_{50} ratio (EC_{50} shift) in the case of L-NAME was less compared to other inhibitors, however, significant difference was observed applying "Student's t-test" at $p<0.05$ (Table **4**).

3.7. Molecular Docking

The docking studies of the compound OXD-Z2 were carried out with L-type Ca^{2+}-channel (1T0J.pdb) and eNOS (3HR4.pdb and 3NOS.pdb) and for muscarinic receptor, the derivative was docked with M_2 receptor (PDB ID 3UON) using V.Life MDS 4.2 software. The various binding interactions of molecules with these receptors are shown in Table **5**. The docking result of the compound revealed that the compound was energetically favourable in terms of dock score especially with Ca^{2+}-channel and muscarinic receptor which was observed to be -49.5629 and -49.2814, kcal/mol respectively than eNOS receptor (3NOS.pdb and 3HR4.pdb which showed docking score of -46.1786 and –41.341 kcal/mol respectively). The binding interaction of the compound was found to be more favourable with M_2 receptor (PDB ID

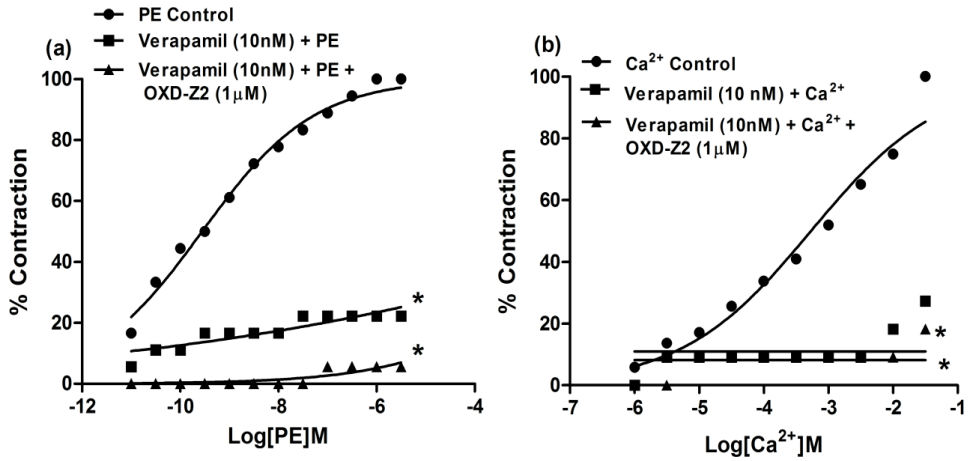

*p<0.05 showed significant difference as compared to control group

Fig. (5). Effect of verapamil alone and in the presence of OXD-Z2 on cumulative concentration-response curves of **(a)** PE and **(b)** Ca^{2+}-induced contraction in rat aortic rings.

Table 4. Effect of OXD-Z2 on vasomotor tonus in presence of various inhibitors.

Inhibitors	Atropine	Methylene Blue	L-NAME	Indomethacin	Glibenclamide
EC_{50} ratio[a]	6.89	8.37	1.04	0.52	0.32

[a]EC_{50} ratio is the ratio of EC_{50} in presence of OXD-Z2 plus inhibitors divided by EC_{50} in presence of OXD-Z2.

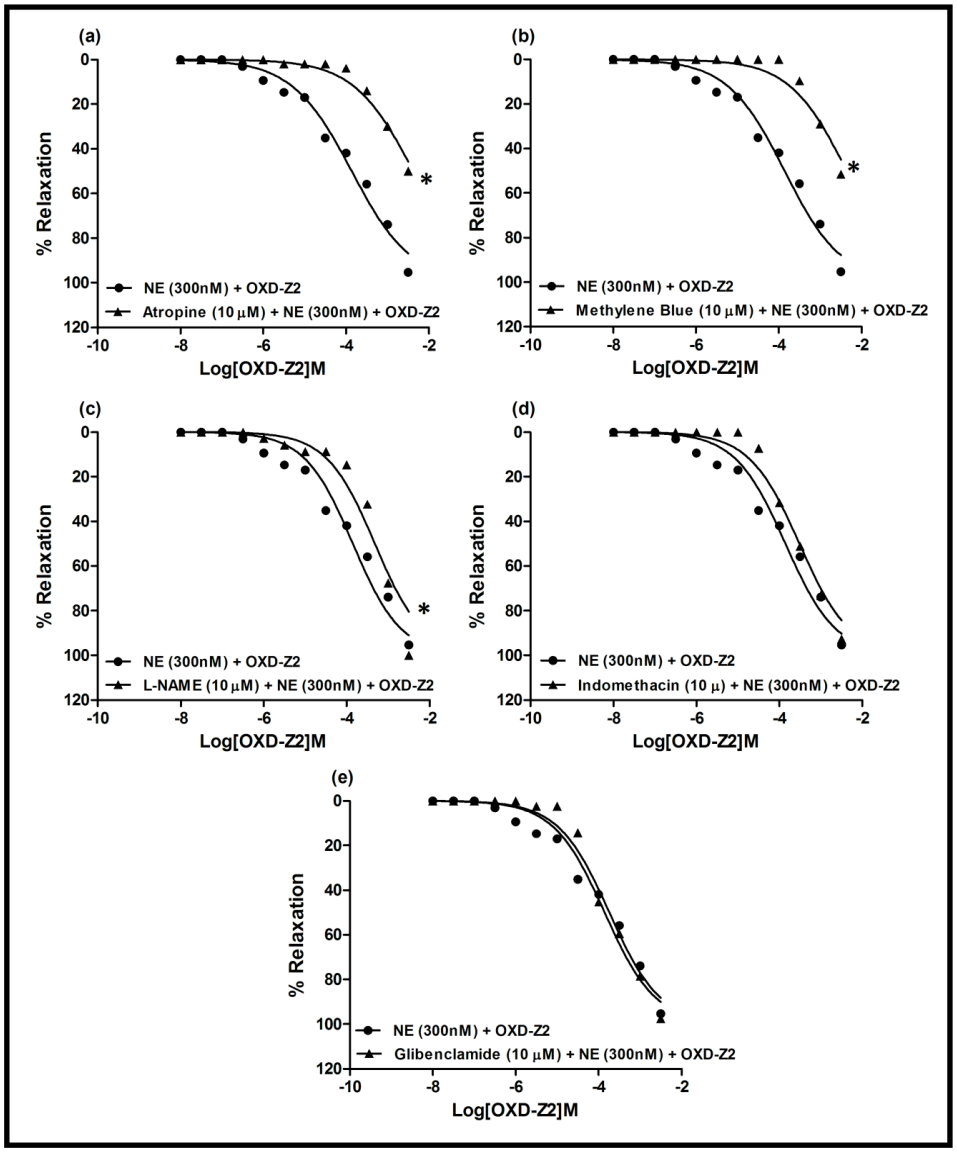

*p<0.05 showed significant difference as compared to control group

Fig. (6). Vasorelaxant effect of OXD-Z2 on NE-induced contraction in rat aortic rings pretreated with inhibitors; (**a**) Atropine, (**b**) Methylene blue, (**c**) L-NAME, (**d**) Indomethacin and (**e**) Glibenclamide.

3UON) which showed the N- of the oxadiazole binds with the amino acid residues, Arg 121A and Lys 383A through hydrogen bonding and whereas C-of the pyridine ring binds with the amino acid residue PHE1004A through π – π stacking (Fig. **7**). Hydrophobic and Van der Waal's interactions were found with various amino acids in the active site of the receptor. These binding interactions reveal the importance of N- of the oxadiazole and C- of the pyridine, so that the better M_2 receptor inhibitory activity was expected. Even though the compound showed favorable binding interactions with all other receptors, the H-bonding interaction was found only with the M_2 receptor. These studies gave us the insight for the development of M_2 receptor inhibitor in future.

4. DISCUSSION AND CONCLUSION

Eight oxadiazole derivatives with different substituents were synthesized. An oxadiazole derivative coded as OXD-Z2 among eight derivatives with a pyridine-3-yl ring attached to carbon (C) in position 5, an acetyl group attached to nitrogen (N) in position 3, and a toluyl group attached to C in position 2 of the oxadiazole ring was chosen to evaluate

Table 5. Amino acids involved in the binding interaction between OXD-Z2-receptor complexes.

PDB ID	Hydrophobic Interaction	Van der Waal Interaction
1T0J	Lys 90A, Ala 335B, Pro 336B, Ile 338B, Glu 381B	Lys 90A, Asp 91A, Phe 92A, Arg 227A
3UON	Val 125A, Arg 121A, Lys 383A, Val 385A	Asn 58A, Arg 121A, Cys 124A, Pro 128A, Arg 135A
3NOS	Asp 444A, Trp 445A, Asn 466A, Cys 99B, Gly 101B, Ser 102B, Asp 444B, Ala 446B, Asn 466B	Gly 101B, Ser 102B, Asp 444A, Trp 445B, Ala 446A, Asn 466A
3HR4	Val 55F, Ala 57F, Glu 67F, Thr 70F, Met 71F, Ala 57H, Asp 58H, Glu 67H	Glu 54F, Val 55F, Ala 57F, Asp 58F

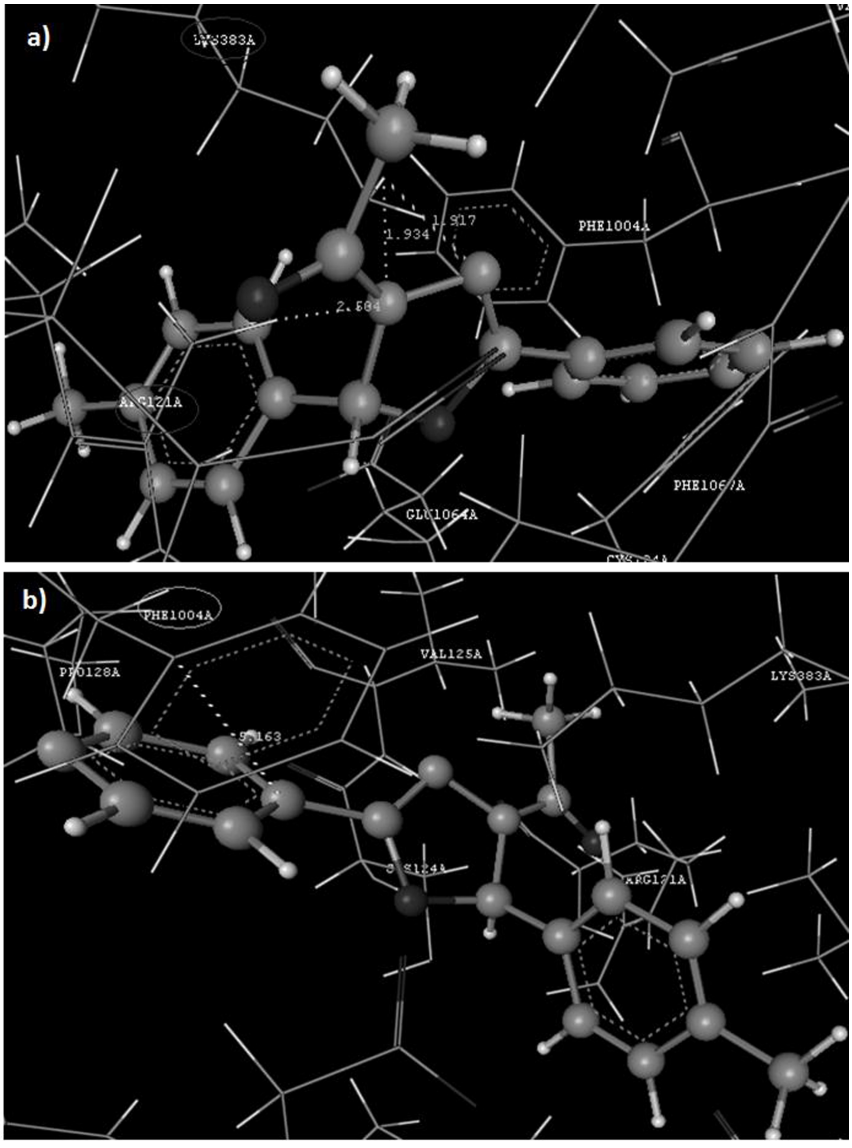

Fig. (7). Binding interactions of OXD-Z2 with 3UON (M_2-muscarinic receptor) in molecular docking studies.

mechanisms of vasorelaxation. OXD-Z2 was found to show vasorelaxant action in phenylephrine (PE), norepinephrine (NE) and KCl pre-contracted rat thoracic aorta with EC_{50} values given in Table **3**. Incubation of the aortic ring with OXD-Z2 shifted the concentration-response curve of PE, NE and KCl towards the right showing inhibition of contraction by OXD-Z2. The vasorelaxation produced by OXD-Z2 was found to be slightly more in endothelium denuded aortic rings than endothelium intact rings but not statistically significant. Thus, it can be inferred from the results that OXD-Z2 induced vasorelaxation may involve both endothelium-dependent and -independent mechanisms. Therefore, a series of *ex vivo* experiments were carried out to explore the mechanism involved in OXD-Z2-induced vasorelaxation.

It is well known that PE and NE act on α-receptors and generate inositol triphosphate (IP_3) and diaceylglycerol (DAG), releasing calcium from intracellular stores and activating protein kinase C, respectively. IP_3 binds to its receptors in the sarcoplasmic reticulum and releases Ca^{2+} to cause contraction and opens receptor-dependent Ca^{2+}-channel. The contraction induced by PE and NE is due to calcium influx either via opening of voltage-dependent Ca^{2+}-channel or receptor-dependent Ca^{2+}-channel [9, 11]. OXD-Z2 was found to non-competitively antagonize PE (selective α_1-adrenoceptor agonist), NE (non-selective α-adrenoceptor agonist) and Ca^{2+}-induced contraction suggesting that its action may be through α- receptor and/or through inhibition of Ca^{2+}-channel. pD2 values (mentioned in the results) indicated non-competitive antagonism. K^+ also plays important role in the regulation of smooth muscle membrane potential. High K^+ induces contraction of smooth muscle because of depolarization of the cell membrane and increased calcium influx through voltage-dependent Ca^{2+}-channels [12]. OXD-Z2 produced vasorelaxation in KCl-precontracted aortic ring, which explained involvement of blockade of voltage-dependent Ca^{2+}-channel in the activity.

Both L-type and non L-type Ca^{2+}-channels are involved in the increase in calcium release during PE and NE-induced contraction [13, 14] and verapamil blocks L-type (voltage-dependent) Ca^{2+}-channel in a concentration-dependent manner [15]. The effect of OXD-Z2 on phenylephrine-induced contraction in aortic rings pretreated with verapamil was studied to investigate the role of L-type Ca^{2+}-channel in vasorelaxation. Pretreatment with verapamil inhibited both PE and Ca^{2+}-induced contractions in the aorta because of the blockade of L-type Ca^{2+}-channels. Incubation of OXD-Z2 along with verapamil further shifted the PE curve towards right but failed to do so in calcium curve. The most probable reason could be that calcium-induced contraction was completely abolished by verapamil and OXD-Z2 could not further alter the contraction. Moreover, OXD-Z2 did not reverse verapamil action as well and thus it can be inferred that OXD-Z2-inhibited L-type Ca^{2+}-channel, leading to aortic vasorelaxation.

The role of Ca^{2+}-channel in OXD-Z2-induced vasorelaxation was observed in the above experiments. Another set of experiments was performed to further explore the role of NO in OXD-Z2 induced vasorelaxation in the endothelium intact aorta. NO, known as endothelium derived relaxing factor (EDRF), is associated with relaxation of blood vessels. Various neuro-humoral and physical stimuli release NO from endothelial cells. Various agents such as acetylcholine, histamine, clonidine and adenosine stimulate specific endothelial receptors and release NO which mediates relaxation. NO activates soluble guanylyl cyclase and then increases the production of cGMP, leading to protein kinase G activation. This inhibits Ca^{2+} influx and produces vasorelaxation [16, 17]. The inhibitors, atropine (muscarinic receptor antagonist), L-NAME (NO synthase inhibitor) and methylene blue (non-selective cGMP inhibitor) were found to inhibit the OXD-Z2-induced relaxation suggesting that OXD-Z2 may mediate relaxation through the release of NO-cGMP pathway by acting on muscarinic receptor [18]. However, glibenclamide did not alter OXD-Z2-induced relaxation, suggesting no role for K^+-channel. However, it was seen earlier that OXD-Z2 inhibited KCl-induced contraction. The above observation indicated that opening of K^+-channel opening may be involved in OXD-Z2-induced vasorelaxation at higher concentrations [19]. Similarly, indomethacin also failed to inhibit OXD-Z2-induced vasorelaxation, indicating that relaxing mediator such as prostanoids is not involved in the OXD-Z2-induced vasorelaxation.

The interaction between OXD-Z2 and various targets were assessed by molecular docking studies. Three targets, L-type Ca^{2+}-channel, muscarinic receptor and eNOS were chosen for docking studies on the basis of the above observations. eNOS was also chosen for molecular docking study, as NO is a key player and OXD-Z2 activity was attenuated in presence of L-NAME. The docking score ranged between -41 to -49, which showed strong binding or interaction between OXD-Z2-receptor complexes. The compound, OXD-Z2 showed hydrogen bonding and π – π stacking with muscarinic receptor.

Thus, it can be deduced from the present *ex vivo* studies on rat aortic rings and *in silico* molecular docking studies that OXD-Z2 is a promising molecule which produces vasorelaxation possibly by dual mechanisms: a) direct inhibition of L-type calcium channel (endothelium-independent) and b) agonistic action on muscarinic receptor through NO-cGMP pathway (endothelium-dependent). However, further studies need to be designed to assess *in vivo* safety and efficacy in suitable animal models in order to prove its usefulness in cardiovascular diseases.

LIST OF ABBREVIATIONS

OXD-Z2 = methyl (toluyl) substituted-1,3,4-oxadiazole

NE = Norepinephrine

PE = Phenylephrine

Ca^{2+} = Calcium

K^+ = Potassium

CRC = Concentration-response curve

CONFLICT OF INTEREST

The authors confirm that this article content has no conflict of interest.

ACKNOWLEDGEMENTS

The authors are thankful to Manipal University for providing the facilities and instruments to perform the experimental studies.

REFERENCE

[1] Endemann, D.H., Schiffrin, E.L. Endothelial dysfunction, *J. Am. Soc. Nephrol.,* **2004**, *15*, 1983-1992.

[2] Esper, R.J., Nordaby, R.A., Vilarino, J.O., Paragano, A., Cacharron, J.L., Machado, R.A. Endothelial dysfunction: a comprehensive appraisal, *Cardiovas. Diabetol.,* **2006**, *5*, 1-18.

[3] Girges, M.M. Synthesis and pharmacological evaluation of novel series of sulfonate ester-containing 1,3,4-oxadiazole derivatives with anticipated hypoglycaemic activity. *Arzneim.-Forsch.,* **1994**, *44*, 490-495.

[4] Mylari, B.L., Beyer, T.A., Scott, P.J., Aldinger, C.E., Dee, M.F., Siegel, T.W., Zembrowski, W.J. Potent, orally active aldose reductase inhibitors related to zopolrestat: surrogates for benzothiazole side chain. *J. Med. Chem.,* **1992**, *35*, 457-465.

[5] Bankar, G.R., Nandakumar, K., Nayak, P.G., Thakur, A., Rao, C.M., Kutty, N.G. Vasorelaxant effect in rat aortic rings through calcium channel blockage: A preliminary *in vitro* assessment of a 1, 3, 4- oxadiazole derivative. *Chem. Biol. Interact.,* **2009**, *181*, 377-382.

[6] Choudhari, P.B., Bhatia, M.S., Jadhav, S.D. Pharmacophore modelling, quantitative structure activity relationship (QSAR) and docking studies of pyrimidine analogs as potential calcium channel blockers. *J. Korean Chem. Soc.,* **2013**, *57*, 99-103.

[7] Rios, M.Y., Lopez-Martinez, S., Lopez-Vallejo, F., Medina-Franco, J.L., Villalobos-Molina, R., Ibarra-Barajas, M., Navarette-Vazquez, G., Hidalgo-Figueroa, S., Hernandez-Abreu, O., Estrada-Soto, S. Vasorelaxant activity of some structurally related triterpenic acids from *Phoradendron reichenbachianum* (Viscaceae) mainly by NO production: *ex vivo* and *in silico* studies. *Fitoterpia,* **2012**, *83*, 1023-1029.

[8] Jakubik, J., Randakova, A., Dolezal, V. On homology modelling of the M_2 muscarinic receptor acetylcholine receptor subtype. *J. Comput. Aided Mol. Des.,* **2013**, *27,* 525-538.

[9] Hong, Z., Hong, F., Olschewski, A., Cabrera, J.A., Varghese, A., Nelson, D.P., Weir, K. Role of store-operated calcium channels and calcium sensitization in normoxic contraction of the ductus arteriosus. *Circulation*, **2006**, *114*, 1372-1379.

[10] Kini, S.G., Bhuva, H.A. Synthesis, anticancer activity and docking of some substituted benzothiazoles as tyrosine kinase inhibitors. *J. Mol. Graph. Model,* **2010**, 29, 32-37.

[11] Maciel, S.S., Dias, K.L., Medeiros, I.A. Calcium mobilization as endothelium-independent mechanism of action involved in the vasorelaxant response induced by the aqueous fraction of the ethanol extract Albizia inopinata G.P. Lewis (AFL) in the rat aorta. *Phytomed.,* **2004**, *11*, 130-134.

[12] Chang, G.J., Lin, T.P., Ko, Y.S., Lin, M.S. Endothelium-dependent and –independent vasorelaxation induced by CIJ-3-2F, a novel benzyl-furoquinoline with antiarrhythmic action, in rat aorta. *Life Sci.,* **2010**, *86*, 869-879.

[13] Van Hove, C.E., Van der Donckt, C., Herman, A.G., Bult, H., Fransen. P. Vasodilator efficacy of nitric oxide depends on mechanisms of intracellular calcium mobilization in mouse aortic smooth muscle cells. *Br. J. Pharmacol.,* **2009**, *158*, 920-930.

[14] Karaki, H., Ozaki, H., Hori, M., Mitsui, S.M., Amano, K., Harada, K., Miyamoto, S., Nakazawa, H., Won, K.J., Sato, K. Calcium movements, distribution, and functions in smooth muscle. *Pharmacol. Rev.,* **1997**, *49*, 157-230.

[15] Cuinas, A., Elies, J., Orallo, F., Campos-Toimil, M. Cyclic AMP relaxation of rat aortic smooth muscle is mediated in part by decrease of depletion of intracellular Ca^{2+} stores and inhibition of capacitative calcium entry. *Vascular Pharmacol.,* **2013**, *58*, 98-104.

[16] Koh, S.B., Kang, M.H., Kim, T.S., Park, H.W., Park, C.G., Seong, Y.H., Seong, H.J. Endothelium-dependent vasodilator and hypotensive effects of Crotalaria sessiliflora in rats. *Biol. Pharm. Bull.,* **2007**, *30*, 48-53.

[17] Kang, D.G., Lee, J.K., Choi, D.H., Sohn, E.J., Moon, M.K., Lee, H.S. Vascular relaxation by the methanol extract of Sorbus cortex via NO-cGMP pathway. *Biol. Pharm. Bull.,* **2005**, *28*, 860-864.

[18] Kim, E., Lee, Y., Rhyu, M. Black cohosh (Cimicifuga racemosa) relaxes the isolated rat thoracic aorta through endothelium dependent and independent mechanisms. *J. Ethnopharmacol.,* **2011**, *138*, 537-542.

[19] Gong, L.L., Fang, L.H., Qin, H.L., Lv, Y., Du, G.H. Analysis of the mechanisms underlying the vasorelaxant action of coptisine in rat aortic rings. *Am. J. Chin. Med.,* **2012**, *40*, 309-320.

Received: April 02, 2015 Revised: September 01, 2015 Accepted: September 11, 2015